Electronic Supplementary Information

Effect of the driving force on nanoparticles growth and shape: an opto-electrochemical study

Jean-Marc Noël, Mathias Miranda Vieira, Vitor Brasiliense, Jean-Francois Lemineur, Catherine Combellas and Frédéric Kanoufi

Description of the videos.

Videos SV1-3 were recorded under dark field illumination in the region of the base of an UME under the following experimental conditions.

Video SV1 : 1mM Fe^{2+} + 0.1M KCl aqueous solution; Au UME biased at E_{UME}=1.2V vs Ag/AgCl for 20s, simultaneously with the beginning of the video.

Video SV2 : 1mM $Fe(bpy)_3^{2+}$ + 0.1M KCl aqueous solution; Au UME biased at E_{UME}=1.2V vs Ag/AgCl for 5s, simultaneously with the beginning of the video.

Video SV3 : 1mM FcMeOH + 50mM KPF_6 aqueous solution; Ag UME biased at E_{UME}=0.7V vs Ag/AgCl for 10s, 2s after the video was started.
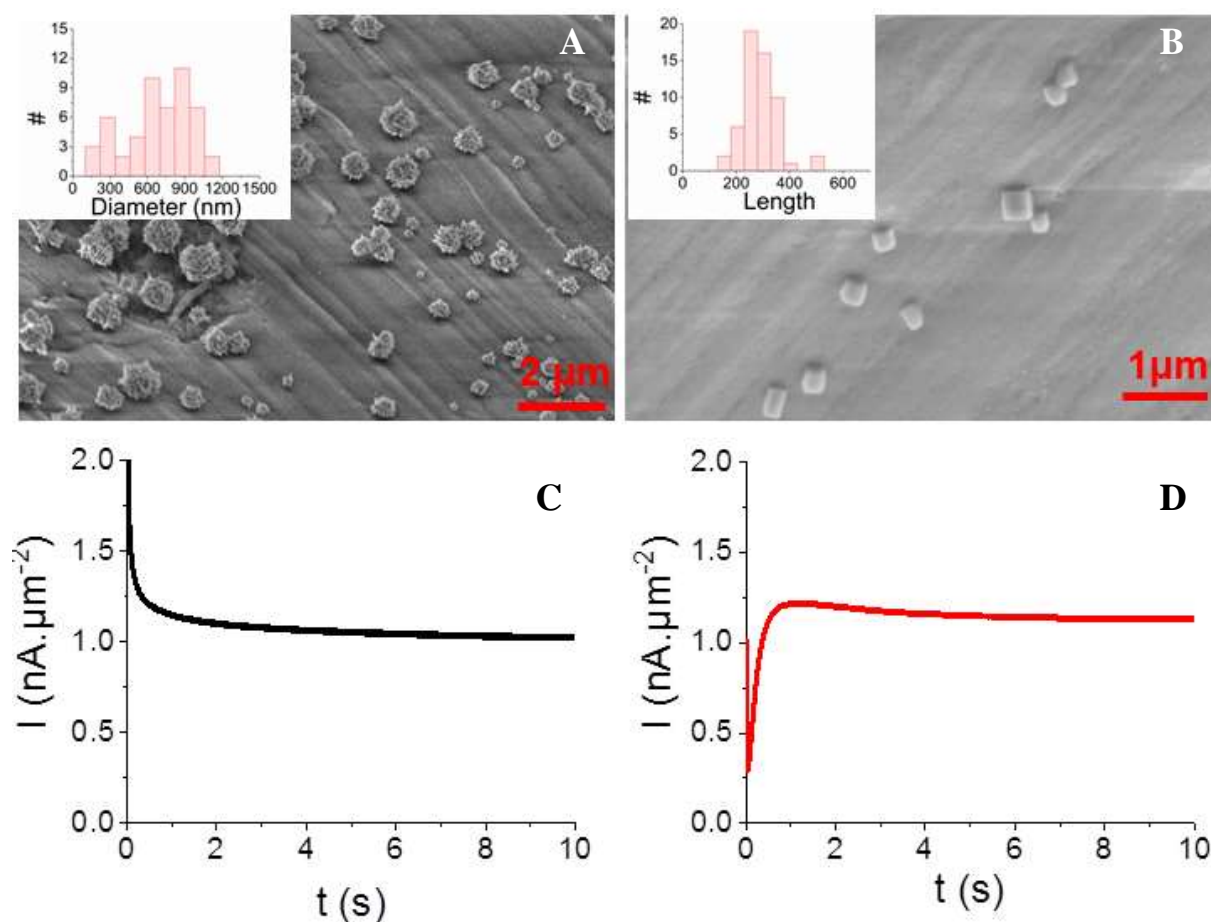
Au NPs SEM images with chronoamperometric curves

Figure S1: A, B) SEM images at the apex of an Au UME recorded after 10s chronoamperometry at $E_{UME} = 1.2V$ vs Ag/AgCl in a 50mM KCl aqueous solution containing A) 1mM $Fe^{II}(SO_4)$, B) 1mM $Fe(bpy)_3^{2+}$. Insets: NP size distributions. C, D) Chronoamperograms recorded at a 25µm diameter Au UME by applying $E_{UME}=1.2V$ vs Ag/AgCl in 0.1M KCl(aq) with (C) 1mM $Fe^{II}(SO_4)$ (−) and (D) 1mM $Fe(bpy)_3^{2+}$ (−).
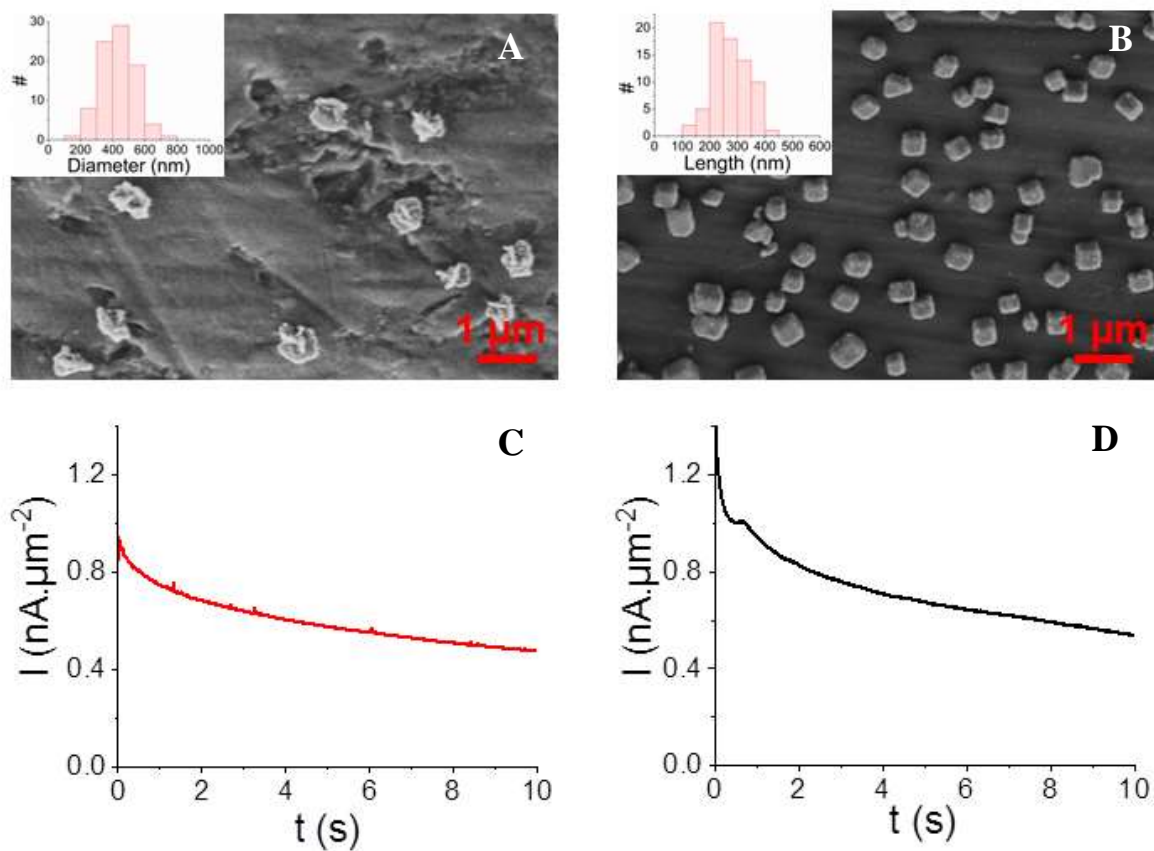
Ag NPs SEM images with chronoamperometric curves

Figure S2: A, B) SEM images at the apex of an Ag UME recorded after 10s chronoamperometry at at $E_{UME=}0.7V$ vs Ag/AgCl in a 50mM KPF$_6$ aqueous solution containing A) 1mM FcMeOH or B) 1mM Fe^{II}(SO$_4$).7H$_2$O. Insets: NP size distributions. C, D) Chronoamperograms recorded at a 25μm diameter Ag UME by applying $E_{UME=}0.7V$ vs Ag/AgCl in 0.1M KCl(aq) with (C) 1mM FcMeOH (−) or (D) 1mM Fe^{II}(SO$_4$) (−).

Voltammetry of Au UME in Fe^{2+} or Fe(bpy)$_3$$^{2+}$ solutions

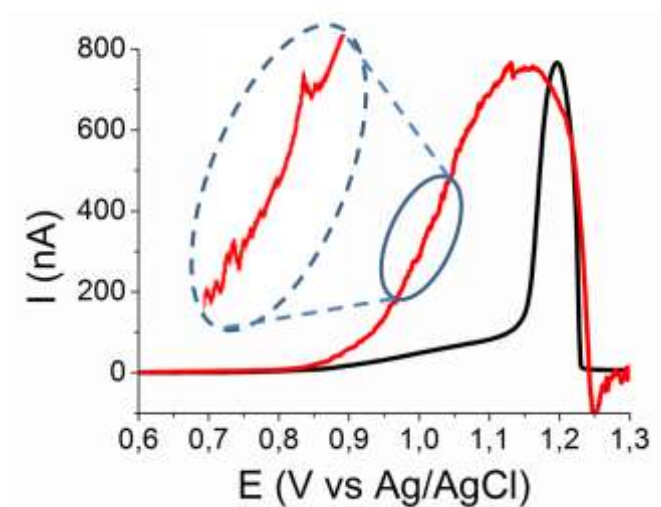**Figure S3:** Linear sweep voltammograms of the oxidation of a 25µm diameter Au UME in 0.1M KCl(aq) in the presence of 50mM Fe(SO$_4$) (−) or 1mM Fe(bpy)$_3$$^{2+}$ (−); scan rate: 50mV.s^{-1}.

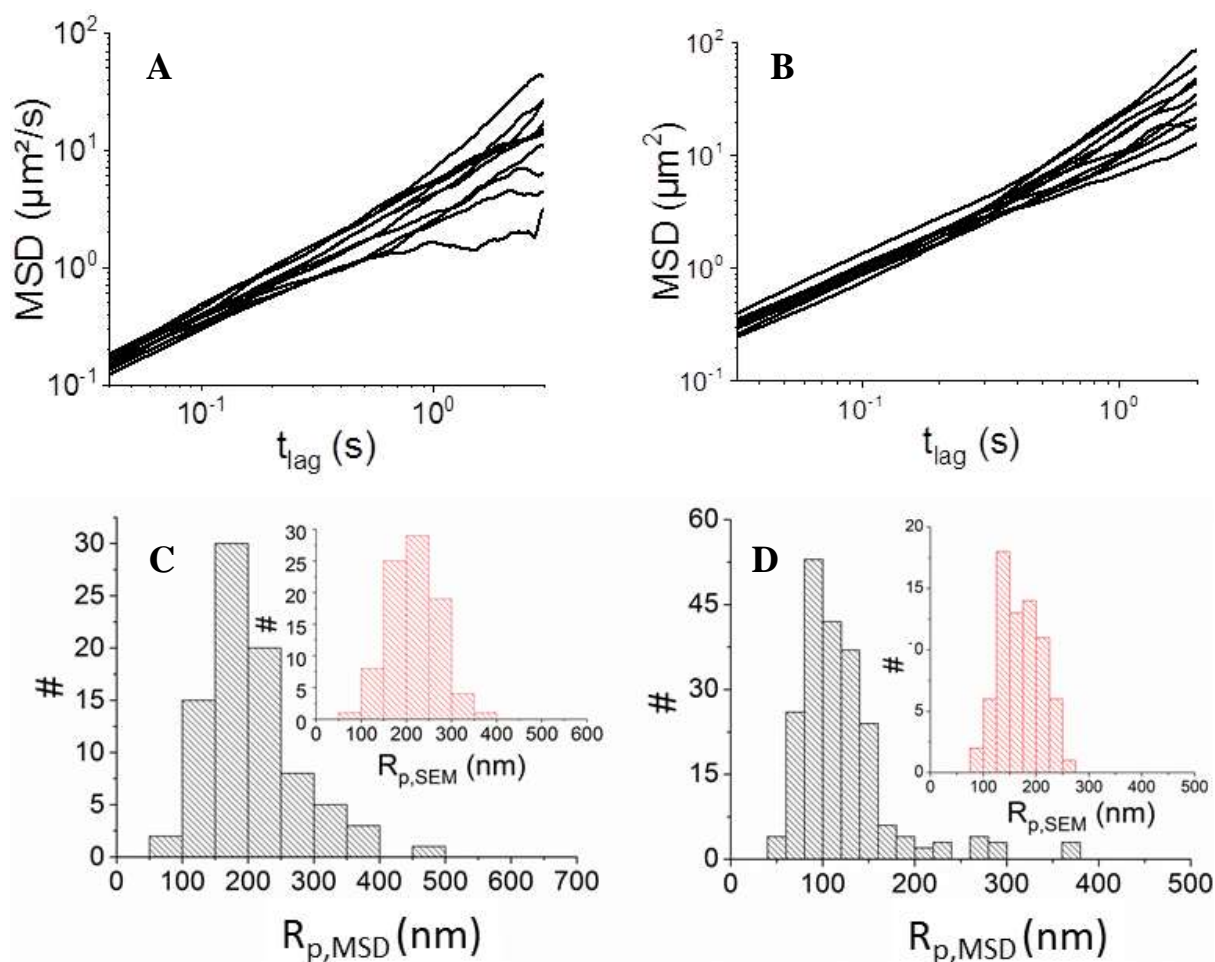**MSD analysis of AgNFs and AgNCs electrogeneration**

Figure S4: A, B) MSD analysis of individual AgNFs and AgNCs trajectories, respectively, during the growth process (from videos SV1 and 2, respectively). C, D) Distribution of the NPs hydrodynamic radius from MSD analysis of individual 2D trajectories for AgNFs and AgNCs, respectively. Insets: distributions of the equivalent radius inferred from SEM images (Figures S2A and B, respectively). $E_{UME=}0.7V$ vs Ag/AgCl.
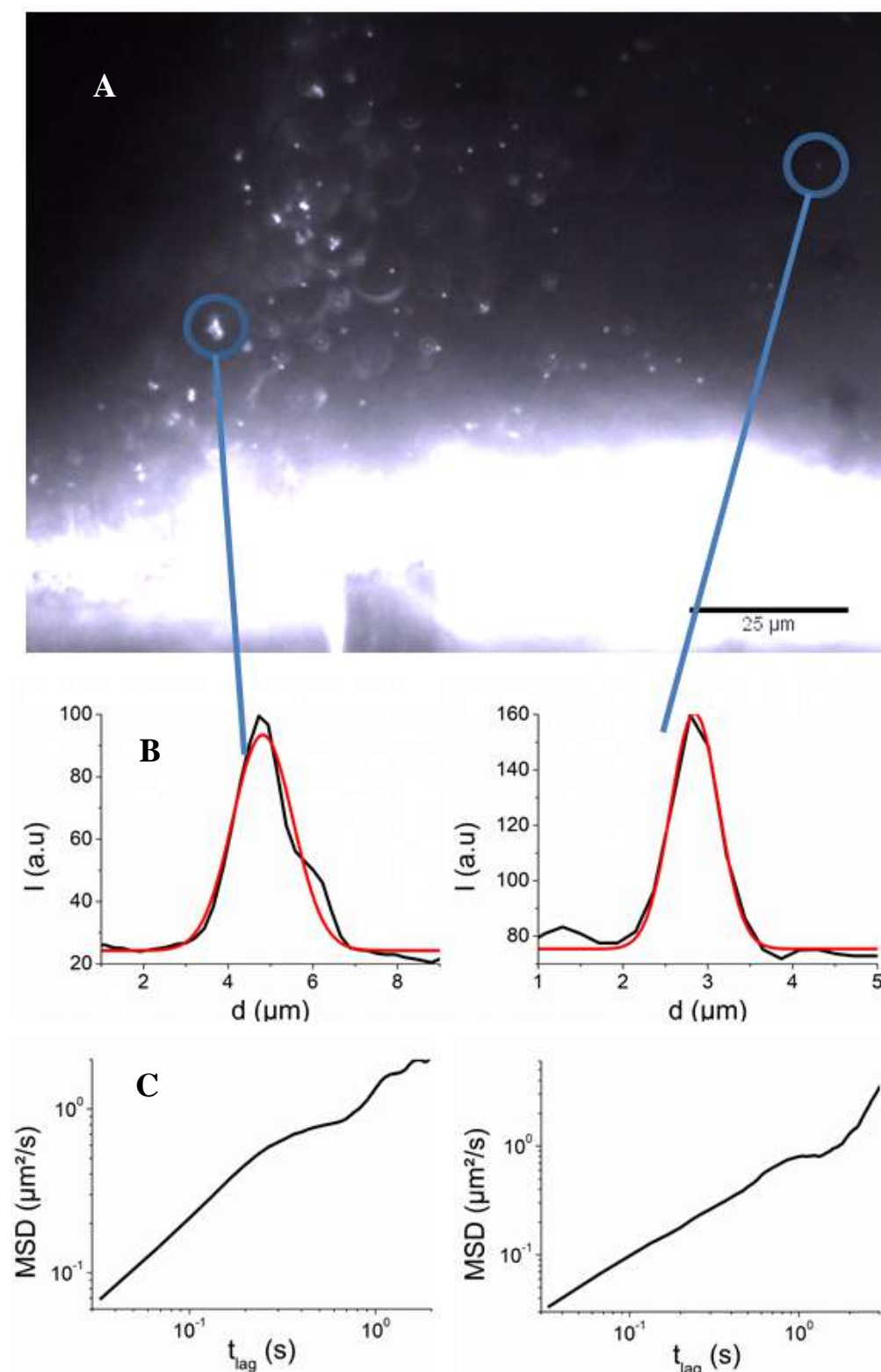
Optical vs MSD particle sizing

Figure S5: A) Dark field optical image (from video SV1) in the region of the base of an Au UME taken 10s after the application of E_{UME}=1.2V vs Ag/AgCl. B) Intensity profiles of 2 AuNFs extracted from A). AuNFs sizes obtained from the FWHM are $R_{p,opt}$=840 (left) and 330 nm (right). C) MSD analysis of the corresponding individual AuNFs provides radii $R_{p,MSD}$=880 (left) and 370 nm (right).
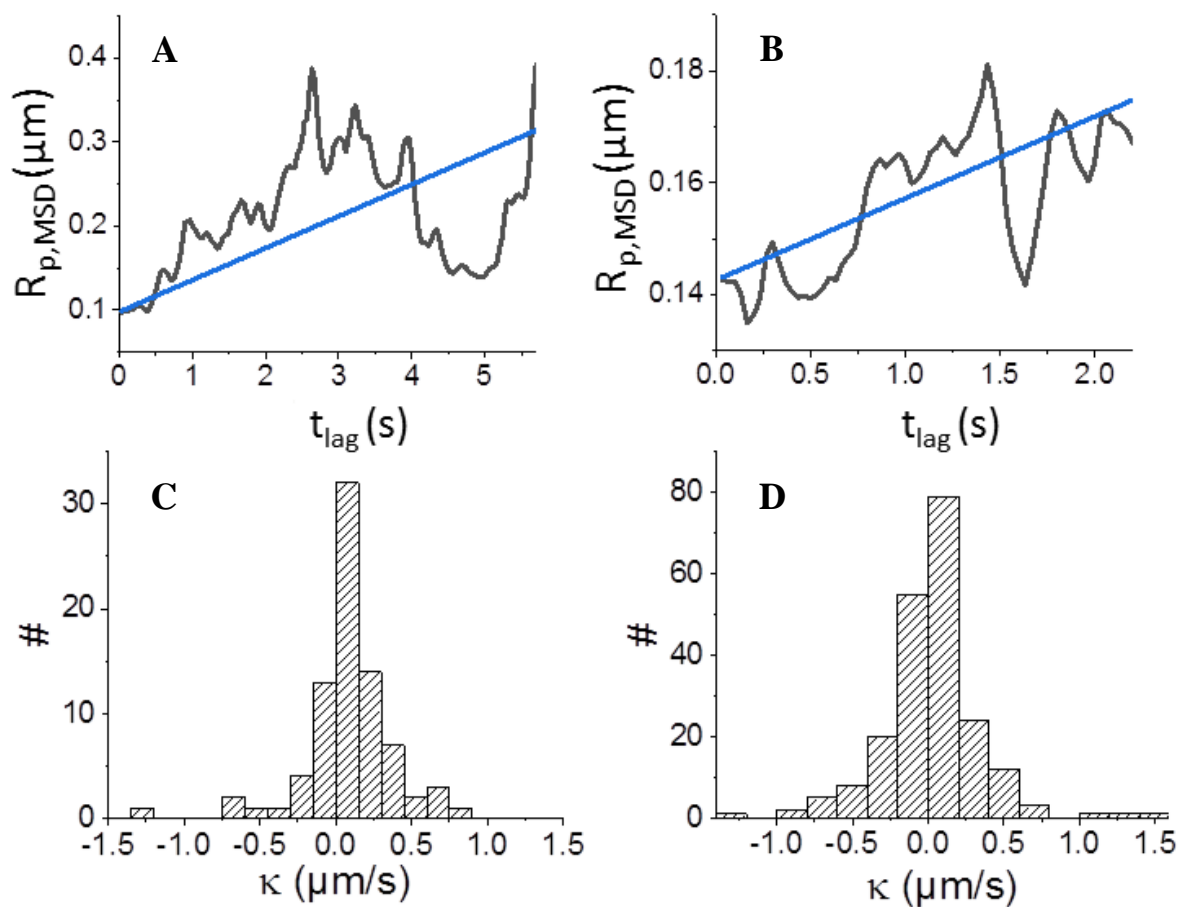
Ag NPs growth rate distributions

Figure S6: A, B) Examples of experimental single Ag NPs instantaneous radius evolution with time (black); fit by A) $\kappa_{AgNF} = 0.5\,\mu m/s$ and B) $\kappa_{AgNC} = 0.01\,\mu m/s$ (blue). C, D) Distribution of κ_{AgNF} and κ_{AgNC} extracted from C) video SV3, and D) the video in reference [1]. Mean κ and associated standard deviation are given in Table 1.
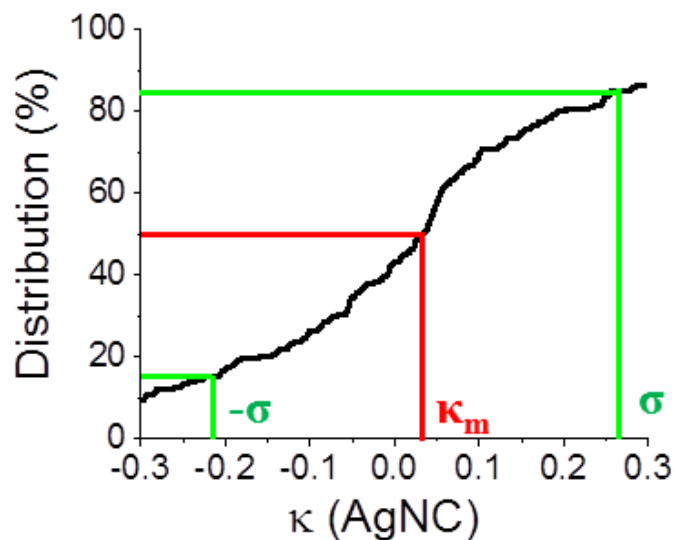
Cumulative frequency growth rates

Figure S7: Example of the cumulative frequency growth rate κ distribution used to extract the median value κ_m (here for κ_{AgNC}) and standard deviation σ determined from the 15% and 85% percentiles of the population. The median values κ_m are given in Table 1 for all the electrosyntheses. The standard errors in Table 1 were determined as $\sigma/\sqrt{N}$ where and N is the number of κ values extracted from the videos.

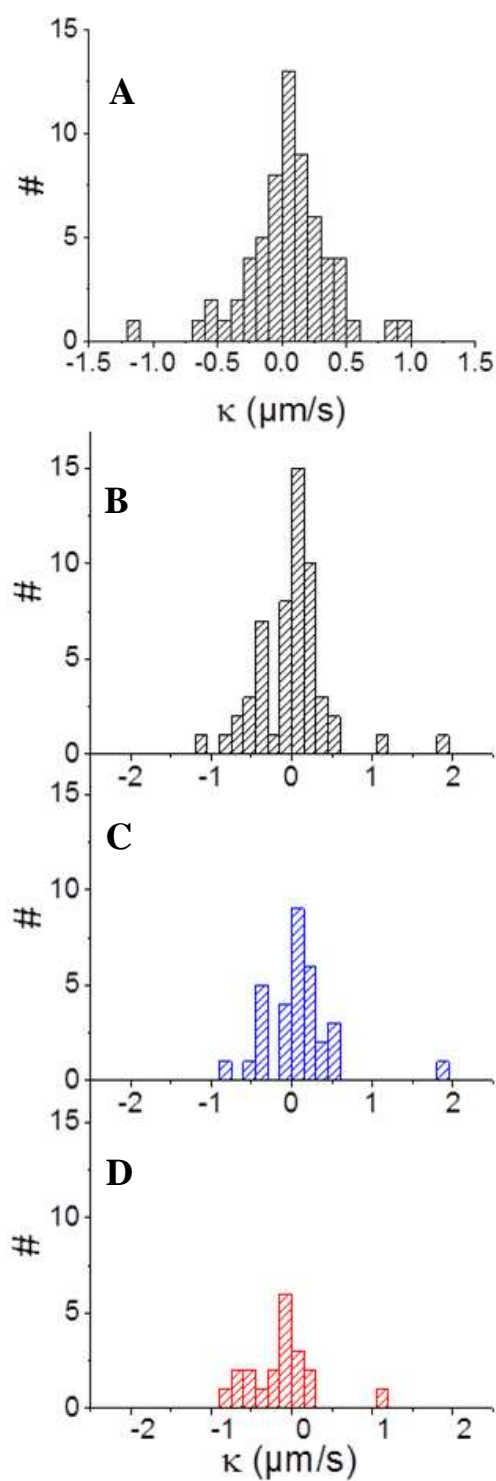**Evidencing the dissolution of AuNC from growth rates distributions**

Figure S8: Distribution of A) κ_{AuNF} and B) κ_{AuNC} extracted from all experimental trajectories of videos SV1 for $R_p < 700$nm and SV2, respectively. Distribution of κ_{AuNC} C) between 0 and 7s and D) from 7s to the end (15s) of video SV2.

Principle of growth rate estimate from MSD analysis

1. Trajectory analysis

Particle growth was deduced from the MSD analysis of single NPs trajectories tracking. Such tracking was obtained from dark field movies such as video SV1. The tracking of individual NPs was performed using ImarisTrack module in the "Autoregressive Motion" mode. After the automatic tracking procedure, all tracks were manually inspected to check they correspond to diffusing particles. At this point, 152 trajectories were recorded. The lengths of the tracked trajectories ranged from 20 to 250 time steps. Only tracks consisting of more than 70 time steps were selected for further MSD segmented analysis, as presented in the main text.
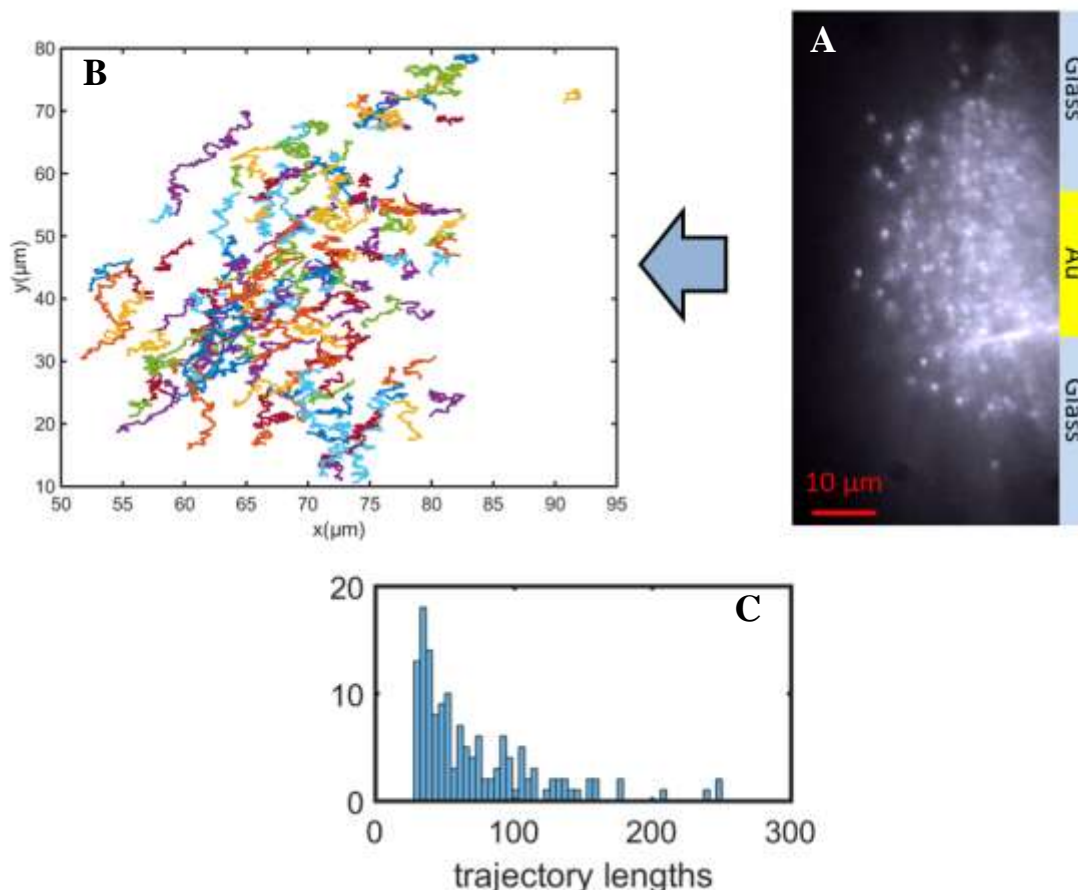

Figure S9.Principle of single NP trajectory tracking. Movies are analyzed using ImarisTrack software: A) raw image (snapshot taken from video SV1) and B) superposition of all the resulting trajectories (each color represents a different trajectory). The spatial scales of Figures A and B are the same. In C) the lengths of the trajectories are represented on a histogram. Only particles tracked for longer than 100 time steps (highlighted in light blue) were considered for the MSD treatment described in section 2.3.

2. Modeling of growing particles

2.1. Kinetic limited growth

Kinetic limited growth was chosen as a limit case under our experimental configuration. This is likely to be the case since nucleation is probably limited by the driving force, as shown from the smaller size of NCs compared to NFs. Then, the diffusive flux of species towards a reactant sphere can be obtained by solving the diffusion equations in spherical coordinates, assuming total consumption of the reactants at the surface of the sphere. It is analogous to the

establishment of the steady state flux or current at a spherical UME.[2] The volume change per unit time can then be obtained as:

$$\frac{dV(t)}{dt} = 4\pi\kappa R^2 \quad \text{or equivalently} \quad \frac{dR(t)}{dt} = \kappa$$

where R is the radius of the NP and κ scales as its growth rate ($\mu m/s$).
The solution of this differential equation yields:

$$R(t) = R_0 + \kappa t$$

with R_0 the initial NP radius at t=0. The time t in the tracking experiment may be the time lag, t=0 being the time when the optical tracking is started (when the NP is detected). The radius then corresponds to the hydrodynamic radius inferred from the MSD analysis. Assuming the instantaneous NP diffusion coefficient $D_{NP}(t)$ is inversely proportional to the instantaneous hydrodynamic radius $R_{p,MSD}(t)$ through the Stokes-Einstein relationship ($D_{NP}=k_BT/6\pi\eta R_{p,MSD}$), $D_{NP}(t)$ can be obtained from the values of $R_{p0,MSD}$ and $D_{NP,0}$ of the NP size and diffusion coefficient at the start of the trajectory (t=0) as:

$$D_{NP}(t) = D_{NP,0} \Big/ \left(1 + \frac{\kappa t}{R_{p0,MSD}}\right)$$

The numerical simulations herein assume this model and aim at determining the physical parameters $R_{p0,MSD}$ and κ from a given trajectory.

2.2. Growth analysis from MSD curve

The MSD analysis of a trajectory reflects the mean diffusion coefficient during the trajectory. It is described elsewhere.[3] Long enough trajectories can be divided in smaller segments, which are analyzed separately via MSD. This procedure allows estimating the average diffusion coefficient on each segment and therefore observing variations of the diffusion coefficient with time, from which the particle growth dynamics is inferred. The procedure is intrinsically stochastic, therefore fluctuations are expected.
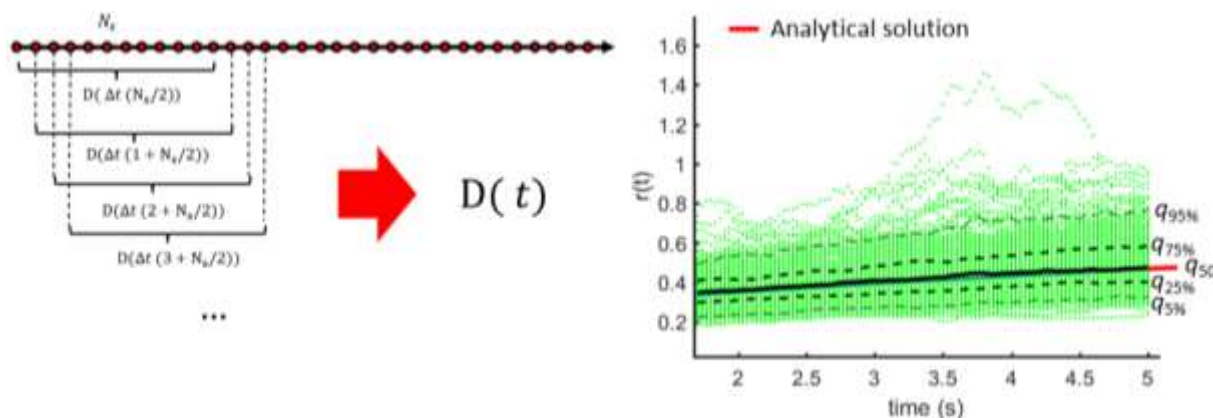
References

[1] V. Brasiliense, J.-M. Noël, K. Wonner, K. Tschulik, C. Combellas and F. Kanoufi, *ChemElectroChem* 2018, **5**, 3016.
[2] A. J. Bard and L. R. Faulkner Eds. In *Electrochemical Methods: Fundamentals and applications*, 2nd Ed., Wiley: New York, 2000, p. 170.
[3] C. Batchelor-McAuley, A. Martinez Marrades, K. Tschulik, A. N. Patel, C. Combellas, F. Kanoufi, G. Tessier and R. G. Compton, *Chem. Phys. Lett.* 2014, **597**, 20.